Applied Numerical Mathematics 62 (2012) 91–111

Contents lists available at SciVerse ScienceDirect

Applied Numerical Mathematics

www.elsevier.com/locate/apnum

Efficient pricing of commodity options with early-exercise under the Ornstein–Uhlenbeck process

B. Zhang [a,*], L.A. Grzelak [a,b], C.W. Oosterlee [a,c]

[a] Delft University of Technology, Mekelweg 4, 2628CD, Delft, The Netherlands
[b] Rabobank International, Utrecht, The Netherlands
[c] CWI – Centrum Wiskunde & Informatica, Amsterdam, The Netherlands

ARTICLE INFO

Article history:
Received 8 March 2011
Received in revised form 21 September 2011
Accepted 3 October 2011
Available online 21 October 2011

Keywords:
Early-exercise commodity options
Efficient pricing
Fourier-cosine expansions
Ornstein–Uhlenbeck process
Error analysis

ABSTRACT

We analyze the efficiency properties of a numerical pricing method based on Fourier-cosine expansions for early-exercise options. We focus on variants of Schwartz' model based on a mean reverting Ornstein–Uhlenbeck process, which is commonly used for modeling commodity prices. This process however does not possess favorable properties for the option pricing method of interest. We therefore propose an approximation of its characteristic function, so that the Fast Fourier Transform can be applied for highest efficiency.

1. Introduction

Computational Finance is one of those mathematical areas in which stochastic modeling and numerical mathematics are closely intertwined. Efficient numerical pricing methods are for example required for financial derivatives, on stocks, interest rates, credit or commodities, all governed by stochastic differential equations. In this paper we focus on a numerical pricing technique for commodity derivatives that can be exercised before the expiration date of the contract.

Movements in the commodity markets expose participants to different types of risks. An obvious way for market players to control their exposure to price and volume fluctuations is by buying or selling derivatives written on the underlying products. Bermudan but also swing options, which allow one to buy or sell extra quantities of a commodity, are commonly sold derivatives with early-exercise features.

Significant contributions have been made in modeling commodity processes by Schwartz and collaborators in [13,16–18] where the authors used a model of Ornstein–Uhlenbeck type [19], which accounts for the mean reversion of prices, combined with a deterministic seasonality component. Often these processes are combined with independent jump components (this extension of the models studied here is straightforward). In this paper we deal with the Fourier-cosine expansion-based COS method [9,10] for pricing early-exercise options under the stochastic processes for commodities. In this method the transitional probability density function is approximated by a Fourier-cosine series expansion, which has a direct relation to the analytically available conditional characteristic function. In [10] it was shown that the COS method can price the early-exercise and barrier options with exponential convergence under various Lévy jump models. The computational

* Corresponding author.
E-mail addresses: Bowen.Zhang@tudelft.nl (B. Zhang), L.A.Grzelak@tudelft.nl (L.A. Grzelak), C.W.Oosterlee@cwi.nl (C.W. Oosterlee).

0168-9274/$36.00
doi:10.1016/j.apnum.2011.10.005

complexity for pricing a Bermudan option with M exercise dates was $O((M-1)N\log_2(N))$, where N denotes the number of terms in the Fourier-cosine expansion.

In the present paper we show that this complexity cannot be easily achieved in the case of mean reverting processes of Ornstein–Uhlenbeck (OU) type. We therefore introduce an *approximation of the original characteristic function*, so that the COS pricing algorithm remains highly efficient for early-exercise commodity options under Ornstein–Uhlenbeck processes, but, at the same time, the error in the option prices is controlled by means of error analysis.

The paper is organized as follows. Details of the OU processes and the COS pricing method are presented in Section 2. In Section 3 the approximate OU model is introduced. It is followed by a detailed error analysis in Section 4; In Section 5 numerical results are presented. Finally conclusions are summarized in Section 6.

2. Problem definition

2.1. The Ornstein–Uhlenbeck process

Stochastic processes for commodities are characterized by the properties of mean reversion and seasonality. If for any reason the price of a certain commodity falls significantly due to overproduction, then market participants expect the price to rise eventually as producers decrease their supply. Moreover, incorporation of seasonality in the model is necessary since energy consumption (the use of electricity, for example) differs in different seasons of the year.

We first look at the OU process without seasonality. The logarithm of the commodity price, $X_t = \log S_t$, is modeled by an Ornstein–Uhlenbeck mean reverting process. We define this process here under a so-called equivalent martingale measure $\mathbb{Q}$,

$$dX_t = \kappa\left(\bar{x}^{\mathbb{Q}} - X_t\right)dt + \sigma\, dW_t^{\mathbb{Q}}, \quad \text{with } X_0 = x_0, \tag{1}$$

with a Brownian motion, $W_t^{\mathbb{Q}}$, is under measure $\mathbb{Q}$ and the parameters κ and σ represent the speed of mean reversion and volatility of the underlying process, respectively. Under this measure, the parameter $\bar{x}^{\mathbb{Q}} := \bar{x} - \lambda$ with λ the market price of risk, and $\bar{x}$ the long-term mean value of the underlying process. In the derivations to follow, we will just use $\bar{x}$ to denote $\bar{x}^{\mathbb{Q}}$.

X_t is normally distributed, i.e.: $X_t \sim \mathcal{N}(\mathbb{E}(X_t), \mathbb{V}\mathrm{ar}(X_t))$, with:

$$\mathbb{E}(X_t|\mathcal{F}_0) = x_0 e^{-\kappa t} + \bar{x}\left(1 - e^{-\kappa t}\right),$$
$$\mathbb{V}\mathrm{ar}(X_t|\mathcal{F}_0) = \frac{\sigma^2}{2\kappa}\left(1 - e^{-2\kappa t}\right).$$

Modeling energy prices by mean reversion is well supported by empirical studies of the price behavior, as described in [2]. General diffusion models that incorporate mean reversion go a long way in capturing the nature of energy prices; notably their tendency to randomly oscillate away from, and over time back towards, a price level determined by the cost of production. These models have gained a more wide-spread acceptance among market practitioners as progress is made in the techniques to estimate the mean reversion level and the mean reversion rates.

We are interested in the characteristic function, $\mathbb{E}(e^{iuX_T}|\mathcal{F}_t)$, related to model (1). Based on [8] the characteristic function is of the form $\phi(u; x_0, \tau) = e^{x_0 B(u,\tau) + A(u,\tau)}$ where $\tau := T - t$; $A(u,\tau)$ and $B(u,\tau)$ satisfy the following set of ODEs:

$$\begin{cases} B'(u,\tau) = -\kappa B, \quad B(u,0) = iu, \\ A'(u,\tau) = \kappa\bar{x}B + \dfrac{1}{2}\sigma^2 B^2, \quad A(u,0) = 0, \end{cases}$$

and the prime $'$ denotes the derivative w.r.t. τ. For the solution we find:

$$\begin{cases} B(u,\tau) = iue^{-\kappa\tau}, \\ A(u,\tau) = \dfrac{1}{4\kappa}\left(e^{-2\kappa\tau} - e^{-\kappa\tau}\right)\left(u^2\sigma^2 + ue^{\kappa\tau}\left(u\sigma^2 - 4i\kappa\bar{x}\right)\right). \end{cases} \tag{2}$$

Then the characteristic function of OU process reads:

$$\phi(u; x_0, \tau) = e^{iux_0 e^{-\kappa\tau} + A(u,\tau)}. \tag{3}$$

2.1.1. Incorporation of seasonality component

More realistic stochastic processes modeling commodity prices include a seasonality component.

As presented in [5,13] we choose a commodity price process, S_t, written as:

$$S_t = e^{g(t)+y_t} = G(t)e^{y_t}, \quad \text{with } S_0 = G(0), \tag{4}$$

where $G(t) \equiv e^{g(t)}$ is a deterministic function which describes the seasonality effect and y_t is a stochastic zero-level-mean reverting process given by:

$$dy_t = -\kappa y_t\,dt + \sigma\,dW_t^y, \quad \text{with } y_0 = 0,$$

with W_t^y a Brownian motion, κ corresponds to the speed of mean reversion and σ determines the volatility. By applying Itô's lemma to Eq. (4), and adding and subtracting $\kappa g(t)$, we obtain the dynamics for S_t of the form:

$$dS_t = \left(\frac{1}{2}\sigma^2 - \kappa\big(y_t + g(t)\big) + \kappa g(t) + g'(t)\right)S_t\,dt + \sigma S_t\,dW_t^y,$$

$g'(t)$ being the derivative of $g(t)$. This equals:

$$dS_t = \left(\frac{1}{2}\sigma^2 - \kappa\log S_t + \kappa g(t) + g'(t)\right)S_t\,dt + \sigma S_t\,dW_t^y.$$

Setting $\theta(t) = g(t) + (\frac{1}{2}\sigma^2 + g'(t))/\kappa$, we arrive at the following process:

$$dS_t = \kappa\big(\theta(t) - \log S_t\big)S_t\,dt + \sigma S_t\,dW_t^y.$$

By taking the log-transform of the stock price, $x_t = \log S_t$, one recognizes the model to be a mean reverting Hull–White model [11], i.e.:

$$dx_t = \kappa\big(\tilde{\theta}(t) - x_t\big)\,dt + \sigma\,dW_t^y, \quad \text{with } x_0 = \log S_0, \tag{5}$$

where $\tilde{\theta}(t) = \theta(t) - \sigma^2/2\kappa$ and $\tilde{\theta}(t) = \bar{x}$ gives the same process as (1). This model is very similar to the model in [3] for electricity prices. The OU process, x_t in (5), admits the solution:

$$x_t = x_0 e^{-\kappa t} + \kappa\int_0^t e^{-\kappa(t-s)}\tilde{\theta}(s)\,ds + \sigma\int_0^t e^{-\kappa(t-s)}\,dW_t^y,$$

and is thus normally distributed, i.e., $x_t \sim \mathcal{N}(\mathbb{E}(x_t), \mathbb{V}\text{ar}(x_t))$, with:

$$\mathbb{E}(x_t|\mathcal{F}_0) = x_0 e^{-\kappa t} + \kappa\int_0^t e^{-\kappa(t-s)}\tilde{\theta}(s)\,ds,$$

$$\mathbb{V}\text{ar}(x_t|\mathcal{F}_0) = \frac{\sigma^2}{2\kappa}\big(1 - e^{-2\kappa t}\big).$$

For process $x_t = \log S_t$, as given by Eq. (5), we find the following ODEs for the characteristic function:

$$\begin{cases} B'(u,\tau) = -\kappa B & \text{with } B(u,0) = iu, \\ A'(u,\tau) = \kappa\tilde{\theta}(t)B(u,\tau) + \dfrac{1}{2}B^2(u,\tau)\sigma^2 & \text{with } A(u,0) = 0, \end{cases}$$

where $\tau = T - t$ for European-style derivatives, and $\tau = t_{m+1} - t, t \in [t_m, t_{m+1}]$, for Bermudan option between any consecutive exercise dates. For the solution we find $B(u,\tau) = iue^{-\kappa\tau}$ and $A(u,\tau)$ contains function $\tilde{\theta}(t)$, which is given by:

$$\tilde{\theta}(t) = \theta(t) - \frac{1}{2}\frac{\sigma^2}{\kappa} = \frac{1}{\kappa}g'(t) + g(t).$$

The ODE for $A(u,\tau)$ admits the following solution:

$$\begin{aligned} A(u,\tau) &= \int_0^\tau A'(u,s)\,ds \\ &= iu\int_0^\tau \big(g'(T-s) + \kappa g(T-s)\big)e^{-\kappa s}\,ds + \frac{1}{4\kappa}u^2\sigma^2\big(e^{-2\kappa\tau} - 1\big). \end{aligned} \tag{6}$$

2.2. The Fourier-cosine method (COS)

The Fourier-cosine pricing method, COS [9,10], is based on the risk-neutral option valuation formula (discounted expected payoff approach):

$$v(x,t_0) = e^{-r\Delta t}\int_{-\infty}^{\infty} v(y,T)\,f(y|x,\Delta t)\,dy, \tag{7}$$

where $v(x,t_0)$ is the present option value, r the interest rate, $\Delta t = T - t_0$ stands for time to maturity, and x, y can be any monotone functions of the underlying asset at initial time t_0 and the expiration date T, respectively. Function $v(y,T)$, which for European option equals the payoff, is known, but the transitional density function, $f(y|x,\Delta t)$, typically is not. Based on Eq. (7), we approximate the conditional density function on a truncated domain, by a truncated Fourier-cosine expansion, which recovers the conditional density function from its characteristic function (see [9]) as follows:

$$f(y|x,\Delta t) \approx \frac{2}{b-a}\sum_{k=0}^{N-1}{}'\,\mathrm{Re}\left(\phi\left(\frac{k\pi}{b-a};x,\Delta t\right)\exp\left(-i\frac{ak\pi}{b-a}\right)\right)\cos\left(k\pi\frac{y-a}{b-a}\right), \tag{8}$$

with $\phi(u;x,\Delta t)$ the characteristic function of $f(y|x,\Delta t)$, a, b determine the truncation interval and Re means taking the real part of the argument. The prime at the sum symbol indicates that the first term in the expansion is multiplied by one-half. The appropriate size of the integration interval can be determined with the help of the cumulants [9].[1]

Replacing $f(y|x,\Delta t)$ by its approximation (8) in Eq. (7) and interchanging integration and summation gives the COS formula for computing the values of European options:

$$v(x,t_0) = e^{-r\Delta t}\sum_{k=0}^{N-1}{}'\,\mathrm{Re}\left(\phi\left(\frac{k\pi}{b-a};x,\Delta t\right)e^{-ik\pi\frac{a}{b-a}}\right)V_k, \tag{9}$$

where

$$V_k = \frac{2}{b-a}\int_a^b v(y,T)\cos\left(k\pi\frac{y-a}{b-a}\right)dy, \tag{10}$$

are the Fourier-cosine coefficients of $v(y,T)$, available in closed form for several payoff functions.

It was found that, with integration interval $[a,b]$ chosen sufficiently wide, the series truncation error dominates the overall error. For conditional density functions $f(y|x,\Delta t) \in C^\infty((a,b)\subset\mathbb{R})$, the method converges exponentially; otherwise convergence is algebraically [10].

Formula (9) also forms the basis for the pricing of Bermudan options [10].

In the present paper, we focus on Bermudan options based on the OU model. The COS pricing method can however be used for various kinds of options as long as the Fourier-cosine coefficients of the option value at maturity and at the early-exercise dates can be determined. This is the case, for instance, for binary, barrier, and swing options.

The pricing method can be used for those underlying processes for which the characteristic function is available, which includes Lévy and affine jump diffusion processes.

2.2.1. Pricing Bermudan options

A Bermudan option can be exercised at pre-specified dates before maturity. The holder receives the exercise payoff when he/she exercises the option. Let t_0 denote the initial time and $\{t_1,\ldots,t_M\}$ be the collection of all exercise dates with $\Delta t := (t_{m+1} - t_m)$, $t_0 < t_1 < \cdots < t_M = T$. The pricing formula for a Bermudan option with M exercise dates then reads, for $m = M-1,\ldots,1$:

$$\begin{cases} c(x,t_m) = e^{-r\Delta t}\displaystyle\int_{\mathbb{R}} v(y,t_{m+1})\,f(y|x,\Delta t)\,dy, \\ v(x,t_m) = \max\big(g(x,t_m),c(x,t_m)\big), \end{cases} \tag{11}$$

followed by

$$v(x,t_0) = e^{-r\Delta t}\int_{\mathbb{R}} v(y,t_1)\,f(y|x,\Delta t)\,dy. \tag{12}$$

[1] So that $|\int_{\mathbb{R}} f(y|x,\Delta t)\,dy - \int_a^b f(y|x,\Delta t)\,dy| < TOL$.

Here x and y are state variables, defined as

$$x := \ln\big(S(t_m)\big) \quad \text{and} \quad y := \ln\big(S(t_{m+1})\big),$$

$v(x,t)$, $c(x,t)$ and $g(x,t)$ are the option value, the continuation value and the payoff at time t, respectively. For call and put options, $g(x,t) \equiv v(x,T)$, with

$$g(x,t) = v(x,T) = \max\big[\alpha\big(e^x - K\big), 0\big], \quad \alpha = \begin{cases} 1 & \text{for a call,} \\ -1 & \text{for a put.} \end{cases} \tag{13}$$

The continuation value in (11) can be calculated by means of the COS formula for different underlying processes:

$$c(x,t_m) := e^{-r\Delta t} \sum_{k=0}^{N-1}{}' \operatorname{Re}\left\{\phi\left(\frac{k\pi}{b-a}; x, \Delta t\right) e^{-ik\pi\frac{a}{b-a}}\right\} V_k(t_{m+1}). \tag{14}$$

Here the function $c(x,t_m)$ represents the approximation of the continuation value.

The idea of pricing Bermudan options by the COS method is to first determine the Fourier-cosine coefficients of the option value at t_1, $V_k(t_1)$, and then insert them into (12). The derivation of an induction formula for $V_k(t_1)$ was the basis of the work in [10]. It is briefly explained here. We start with $V_k(t_M)$ which is obtained by substituting (13) into (10). Then at each time step $t_m, m = M-1,\ldots,1$, $V_k(t_m)$ is recovered in terms of $V_k(t_{m+1})$.

First, the *early-exercise point*, x_m^*, at time t_m, which is the point where the continuation value equals the payoff, i.e., $c(x_m^*, t_m) = g(x_m^*, t_m)$, is determined for example by Newton's method.

At time step t_m, $m = M-2,\ldots,1$, we start with initial guess $x_m^0 := x_{m+1}^0$ (and $x_{M-1}^0 := \log(K)$). We iterate as follows

$$x_m^{n+1} = x_m^n - \frac{c(x_m^n, t_m) - g(x_m^n, t_m)}{c'(x_m^n, t_m) - g'(x_m^n, t_m)},$$

where

$$c'(x,t_m) := e^{-r\Delta t} \sum_{k=0}^{N-1}{}' \operatorname{Re}\left\{\phi\left(\frac{k\pi}{b-a}; x, \Delta t\right) e^{-ik\pi\frac{a}{b-a}} \frac{ik\pi}{b-a} e^{-\kappa\Delta t}\right\} V_k(t_{m+1}),$$

and $g'(x,t_m)$ follows directly from (13). The iteration procedure is continued until error $|\epsilon_n| < TOL$ and $x_m^* := x_m^n$.

The Newton method converges quadratically, i.e., $|\epsilon_{n+1}| \leqslant \bar{P}\epsilon_n^2$. With the initial guess we proposed, the error is sufficiently small ($O(10^{-7})$) after 4 Newton steps, and $O(10^{-10})$ after 5 iterations. In our implementation we prescribe 5 iterations.

Based on x_m^*, we can split $V_k(t_m)$ into two parts: One on the interval $[a, x_m^*]$ and another on $(x_m^*, b]$, i.e.

$$V_k(t_m) = \begin{cases} C_k(a, x_m^*, t_m) + G_k(x_m^*, b, t_m), & \text{for a call,} \\ G_k(a, x_m^*, t_m) + C_k(x_m^*, b, t_m), & \text{for a put,} \end{cases} \tag{15}$$

for $m = M-1, M-2,\ldots,1$, and

$$V_k(t_M) = \begin{cases} G_k(0, b, t_M), & \text{for a call,} \\ G_k(a, 0, t_M), & \text{for a put,} \end{cases} \tag{16}$$

whereby

$$G_k(x_1, x_2, t_m) := \frac{2}{b-a} \int_{x_1}^{x_2} g(x,t_m) \cos\left(k\pi\frac{x-a}{b-a}\right) dx, \tag{17}$$

and

$$C_k(x_1, x_2, t_m) := \frac{2}{b-a} \int_{x_1}^{x_2} c(x,t_m) \cos\left(k\pi\frac{x-a}{b-a}\right) dx. \tag{18}$$

For all $k = 0, 1,\ldots,N-1$ and $m = 1, 2,\ldots,M$, $G_k(x_1, x_2, t_m)$ in (17) is found analytically.

The properties a characteristic function should satisfy for the efficient computation of $C_k(x_1, x_2, t_m)$ (18) are given below and in Lemma 2.1.

The conditional characteristic function between two time points $s < t$ is defined by

$$\begin{aligned}\phi(u; x, t-s) &:= \mathbf{E}\big(e^{iuX_t}|X_s\big)\\ &= \int_{\mathbf{R}} e^{iuy} f(X_t = y|X_s = x, t-s)\,dy\\ &= e^{iux}\int_{\mathbf{R}} e^{iu(y-x)} f\big(X_t = x + (y-x)|X_s = x, t-s\big)\,dy. \end{aligned} \tag{19}$$

We transform $z := y - x$, which gives

$$\phi(u; x, t-s) = e^{iux}\int_{\mathbf{R}} e^{iuz} f(X_t - X_s = z|X_s = x, t-s)\,dz. \tag{20}$$

For underlying processes with independent and stationary increments, like the exponential Lévy processes, the density $f(X_t - X_s = z|X_s = x, t-s)$ only depends on $\Delta t = t - s$, and is independent of x. As a result the characteristic function is of the form

$$\phi(u; x, \Delta t) = \mathrm{e}^{iux\beta}\varphi(u; \Delta t), \tag{21}$$

with $\beta = 1$. Examples of such processes are Geometric Brownian Motion, jump diffusion processes by Kou [12] or Merton [15], and infinite activity Lévy processes [6], like Variance-Gamma (VG) [14], Normal Inverse Gaussian (NIG) [1] or CGMY [4].

From Eq. (3) we have seen that the characteristic function of the OU process can also be written in the form (21), however, with $\beta = e^{-\kappa\Delta t}$ and $\varphi(u; \Delta t) = \exp(A(u, \Delta t))$ defined by (2) or (6). However, OU processes are not governed by the property of independent and stationary increments as the increment does not only depend on Δt, but also on x.

In the lemma to follow we will show that a process with independent and stationary increments, i.e. with $\beta = 1$ in (21), is beneficial for pricing Bermudan options by the COS method as the Fast Fourier Transform can be applied.

Lemma 2.1 *(Efficient computation). The terms $C_k(x_1, x_2, t_m)$ can be computed in $O(N \log_2 N)$ operations, if the stochastic process for the underlying is governed by the general characteristic function* (21) *with parameter $\beta = 1$.*

Proof. At time t_m, $m = 1, 2, \ldots, M$, from Eqs. (9) and (11) we obtain an approximation for $c(x, t_m)$, the continuation value at t_m, which is inserted into (18). Interchanging summation and integration gives the following coefficients, $C_k(x_1, x_2, t_m)$:

$$C_k(x_1, x_2, t_m) := e^{-r\Delta t}\sum_{j=0}^{N-1}{}' \mathrm{Re}\left(\varphi\left(\frac{j\pi}{b-a}; \Delta t\right) V_j(t_{m+1}) \cdot H_{k,j}(x_1, x_2)\right), \tag{22}$$

where $\varphi(u; \tau)$ comes from the general expression for the characteristic function (21). To get $C_k(x_1, x_2, t_m)$, the following integrals need to be computed:

$$H_{k,j}(x_1, x_2) = \frac{2}{b-a}\int_{x_1}^{x_2} e^{ij\pi\frac{\beta x - a}{b-a}} \cos\left(k\pi\frac{x-a}{b-a}\right) dx,$$

with β defined in (21).

From basic calculus, we can split $H_{k,j}(x_1, x_2)$ into two parts as

$$H_{k,j}(x_1, x_2) = -\frac{i}{\pi}\big(H^s_{k,j}(x_1, x_2) + H^c_{k,j}(x_1, x_2)\big),$$

where

$$H^c_{k,j}(x_1, x_2) = \begin{cases} \frac{(x_2 - x_1)\pi i}{b-a}, & \text{if } k = j = 0,\\ \frac{1}{(j\beta + k)}\left[\exp\left(\frac{((j\beta+k)x_2 - (j+k)a)\pi i}{b-a}\right) - \exp\left(\frac{((j\beta+k)x_1 - (j+k)a)\pi i}{b-a}\right)\right], & \text{otherwise,}\end{cases} \tag{23}$$

and

$$H^s_{k,j}(x_1, x_2) = \begin{cases} \frac{(x_2 - x_1)\pi i}{b-a}, & \text{if } k = j = 0,\\ \frac{1}{(j\beta - k)}\left[\exp\left(\frac{((j\beta-k)x_2 - (j-k)a)\pi i}{b-a}\right) - \exp\left(\frac{((j\beta-k)x_1 - (j-k)a)\pi i}{b-a}\right)\right], & \text{otherwise.}\end{cases} \tag{24}$$

Then to determine the value of $C_k(x_1, x_2, t_m)$, we have to compute:

$$C_k(x_1, x_2, t_m) = \frac{-ie^{-r\Delta t}}{\pi} \sum_{j=0}^{N-1}{}' \operatorname{Re}\left(\varphi\left(\frac{j\pi}{b-a}, \Delta t\right) V_j(t_{m+1})\right. \tag{25}$$

$$\left. \cdot \left(H^c_{k,j}(x_1, x_2) + H^s_{k,j}(x_1, x_2)\right)\right), \tag{26}$$

Matrices $H_s := \{H^s_{k,j}(x_1, x_2)\}_{k,j=0}^{N-1}$ and $H_c := \{H^c_{k,j}(x_1, x_2)\}_{k,j=0}^{N-1}$ have a Toeplitz or Hankel structure, respectively, if and only if for all k, j, x_1, x_2, $H^s_{k,j}(x_1, x_2) = H^s_{k+1,j+1}(x_1, x_2)$, and $H^c_{k,j}(x_1, x_2) = H^c_{k+1,j-1}(x_1, x_2)$, which is for $\beta \equiv 1$. Then, the Fast Fourier Transform can be applied directly for highly efficient matrix-vector multiplication [10], and the resulting computational complexity for $C_k(x_1, x_2, t_m)$ is $O(N \log_2 N)$. □

We obtain however terms of the form $j\beta - k$, $j\beta + k$ in the matrix elements in (23) and (24), where $\beta = e^{-\kappa\Delta t}$ for the OU process, instead of terms with $j-k$, $j+k$, for the Lévy jump processes in [10]. In particular, the term $1/(j\beta \pm k)$ cannot be decomposed in terms $j \pm k$, j and/or k, so that we cannot formulate H_s, H_c in terms of Hankel and Toeplitz matrices. This hampers an efficient computation of the matrix-vector products, leading to computations of $O(N^2)$ complexity.

In the next section we will therefore introduce *an approximate OU model* so that the efficient pricing technique with FFT can be applied.

3. An approximate OU model

In this section we introduce an approximation for the characteristic function of the OU processes from Section 2, so that the performance of the COS method for Bermudan options can be improved in terms of computational complexity. The aim is to make use of the FFT algorithm as much as possible with a modified characteristic function. Without loss of generality, we will focus on Bermudan put options here.

The original characteristic functions of the OU processes with and without seasonality can be written as:

$$\phi_{ou}(u; x, \Delta t) = e^{iux} e^{A(u,\Delta t) - iux(1-e^{-\kappa\Delta t})} =: e^{iux}\psi(u; x, \Delta t). \tag{27}$$

Without seasonality we have:

$$A(u, \Delta t) = \frac{1}{4\kappa}\left(e^{-2\kappa\Delta t} - e^{-\kappa\Delta t}\right)\left(u^2\sigma^2 + ue^{\kappa\Delta t}\left(u\sigma^2 - 4i\kappa\bar{x}\right)\right),$$

and with seasonality:

$$A(u, \tau) = iu\int_0^\tau \left(g'(T-s) + \kappa g(T-s)\right)e^{-\kappa s}\,ds + \frac{1}{4\kappa}u^2\sigma^2\left(e^{-2\kappa\tau} - 1\right).$$

The Fast Fourier Transform can be used in the computation of Fourier coefficients $C_k(x_1, x_2, t_m)$, when $\psi(u; x, \Delta t)$ in (27) is approximated by another function, which does not contain variable x. The (approximate) characteristic function is then of the form (21) with $\beta = 1$. We denote by $\phi_{app}(u; x, \Delta t)$ this approximate characteristic function. The approximation suggested here reads

$$\phi_{app}(u; x, \Delta t) := e^{iux}\psi\left(u; \mathbb{E}(x|\mathcal{F}_0), \Delta t\right). \tag{28}$$

In other words, Eq. (20) is replaced by

$$\phi_{app}(u; x, t-s) := e^{iux}\int_{\mathbf{R}} e^{iuz} f\left(X_t - X_s = z | X_s = \mathbf{E}(x|\mathcal{F}_0), t-s\right) dz.$$

This approximation may not be accurate for all model parameters, when pricing Bermudan options. Comparison of the original characteristic function (27) with this approximation (28) gives us that

$$\phi_{app}(u; x, \Delta t) = \phi_{ou}(u; x, \Delta t)e^{iu\epsilon_1}, \tag{29}$$

where ϵ_1 reads

$$\epsilon_1 = \left(x - \mathbb{E}(x)\right)\left(1 - e^{-\kappa\Delta t}\right). \tag{30}$$

Based on (29) the approximation proposed may only be considered accurate for sets of model parameters for which ϵ_1 in (30) is less than a prescribed tolerance level. This tolerance level is defined so that the Bermudan option prices resulting

from the approximate characteristic function at each time step are accurate up to a basis point compared to the option prices obtained by the original characteristic function of the OU process.

The tolerance level for ϵ_1, as well as the requirements model parameters should satisfy so that the approximate characteristic function (28) is accurate and thus the Fast Fourier Transform can be used at each time step, are determined by an error analysis in the next section.

4. Error analysis

Our aim is to keep the error, defined as the difference between Bermudan option values calculated with the original characteristic function and those obtained with x_t approximated by $\mathbb{E}(x_t)$ in $\psi(u; x_t, \Delta t)$ in (27), less than a basis point, which is 1/100-th of a percentage point. Here we discuss how the error in the option value can be controlled and the basis point precision can be achieved.

We first introduce the following notation:

- $\epsilon_c(x,t)$ is the error in the continuation value $c(x,t)$ at time t.
- $\epsilon_x(t)$ is the error in early-exercise point x^* at time t.
- $\epsilon_V(t)$ is the error in V_k at time t, i.e. the error in the Fourier-cosine coefficients of option value $v(x,t)$.

We focus here on the error in Bermudan option values resulting from our approximate characteristic function. For convergence analysis of the COS pricing method we refer the reader to [9] and [10].

4.1. The first step in the backward recursion

The first step in the backward recursion is from $t_M \equiv T$ to t_{M-1}. The *error* in the characteristic function, due to the approximation, gives an error in the continuation value, $c(x, t_{M-1})$, as well as a *shift* in the early-exercise point, $x^*_{t_{M-1}}$. These errors contribute to $\epsilon_V(t_{M-1})$, the error in $V_k(t_{M-1})$.

The connection between the error in the continuation value and the error in the characteristic function is presented in the following lemma.

Lemma 4.1. *The error in continuation value reads*

$$\epsilon_c(x, t_{M-1}) = c\big(x + e^{\kappa\Delta t}\epsilon_1, t_{M-1}\big) - c(x, t_{M-1}), \tag{31}$$

with ϵ_1 defined in (30)*.*

Proof. Applying (27) and (29) gives us:

$$\begin{aligned}\phi_{app}(u; x, \Delta t) &= \exp\big(iuxe^{-\kappa\Delta t} + A(u) + iue^{-\kappa\Delta t}\big(e^{\kappa\Delta t}\epsilon_1\big)\big)\\ &= \exp\big(iu\big(x + e^{\kappa\Delta t}\epsilon_1\big)e^{-\kappa\Delta t} + A(u)\big)\\ &= \phi_{ou}\big(u; x + e^{\kappa\Delta t}\epsilon_1, \Delta t\big).\end{aligned} \tag{32}$$

By substituting (32) in the COS pricing formula (9), we obtain:

$$\hat{c}(x, t_{M-1}) = c\big(x + e^{\kappa\Delta t}\epsilon_1, t_{M-1}\big),$$

which results in:

$$\epsilon_c(x, t_{M-1}) = c\big(x + e^{\kappa\Delta t}\epsilon_1, t_{M-1}\big) - c(x, t_{M-1}). \qquad \square$$

Then we have the next corollary.

Corollary 4.1. *For put options, if $\epsilon_1 > 0$, then $\epsilon_c(x, t_{M-1}) < 0\ \forall x$, and subsequently $\epsilon_x(t_{M-1}) > 0$, and vice versa if $\epsilon_1 < 0$.*

Proof. The continuation value, $c(x,t)$, is a decreasing function for put options. This implies that, for $\epsilon_1 > 0$,

$$\epsilon_c(x, t_{M-1}) := c\big(x + e^{\kappa\Delta t}\epsilon_1, t_{M-1}\big) - c(x, t_{M-1}) < 0.$$

In this case, we have that at the early-exercise point related to the original characteristic function, $x^*_{t_{M-1}}$:

$$\hat{c}\big(x^*_{t_{M-1}}, t_{M-1}\big) < c\big(x^*_{t_{M-1}}, t_{M-1}\big) = g\big(x^*_{t_{M-1}}, t_{M-1}\big).$$

So, the continuation value is smaller than the payoff. Therefore, the approximate early-exercise point is larger than the original $x^*_{t_{M-1}}$ and thus $\epsilon_x(t_{M-1}) > 0$.

For $\epsilon_1 < 0$, $\forall x$, the proof that for $\epsilon_c(x, t_{M-1}) > 0$ $\forall x$, and that $\epsilon_x(t_{M-1}) < 0$ goes similarly. □

The upper bounds of $|\epsilon_c(x, t_{M-1})|$ and $|\epsilon_x(t_{M-1})|$ are found in the next lemma.

Lemma 4.2. *$\forall x$ in the range of integration $[a, b]$, $\forall t$, we have that*

$$\left|c\left(x + e^{\kappa \Delta t}\epsilon_1, t\right) - c(x, t)\right| \leqslant e^a e^{\kappa \Delta t}|\epsilon_1| =: \hat{\epsilon}_c, \tag{33}$$

which implies:

$$\left|\epsilon_c(x, t_{M-1})\right| \leqslant \hat{\epsilon}_c, \quad \forall x \in [a, b]. \tag{34}$$

Error $|\epsilon_x(t_{M-1})|$ can furthermore be bounded in terms of $\hat{\epsilon}_c$.

Proof. Application of Lagrange's mean value theorem, gives

$$\left|c\left(x + e^{\kappa \Delta t}\epsilon_1, t\right) - c(x, t)\right| = e^{\kappa \Delta t}|\epsilon_1|\left|\frac{\partial c(x, t)}{\partial x}\bigg|_{x=\delta_0}\right|, \tag{35}$$

where $\delta_0 \in (x, x + e^{\kappa \Delta t}\epsilon_1)$. The function $\partial c(x, t)/\partial x$ is a non-positive and non-decreasing[2] function for $x \geqslant \log(K)$ for Bermudan put options, which goes to zero as $x \to \infty$. Therefore, if $a \geqslant \log(K)$, we have

$$\max_{x \in [a,b]}\left|\frac{\partial c(x, t)}{\partial x}\right| = \left|\frac{\partial c(x, t)}{\partial x}\bigg|_{x=a}\right|. \tag{36}$$

We denote this derivative of the continuation value at a by $c'(a, t)$, and:

$$\left|c\left(x + e^{\kappa \Delta t}\epsilon_1, t\right) - c(x, t)\right| \leqslant e^{\kappa \Delta t}|\epsilon_1|\left|c'(a, t)\right|. \tag{37}$$

If $a < \log(K)$ Eq. (36) is not valid and the upper bound is $|c'(K, t)|$. However, it overestimates the error in the option value (that is, in Eq. (63)). For example, if x is very small then for the complete integration range $[a, b]$ we will deal with the payoff (not the continuation value) and the error is zero. Therefore we still use $|c'(a, t)|$ for $a < \log(K)$ which works well in all our numerical experiments. At each time step we have $|c'(x, t)| \leqslant |g'(x, t)|$ for $x < \log(K)$. So, if $a < \log(K)$ we have

$$\left|c'(a, t)\right| \leqslant \left|g'(a, t)\right| = e^a. \tag{38}$$

For deep out-of-the money options where $a \geqslant \log(K)$ we find

$$\left|c'(a, t)\right| \leqslant \left|c'\left(\log(K) - 1, t\right)\right| \leqslant \left|g'\left(\log(K) - 1, t\right)\right| = e^{\log(K)-1} \leqslant e^a. \tag{39}$$

Summarizing, we find for all cases:

$$\left|c'(a, t)\right| \leqslant e^a. \tag{40}$$

Substitution of (40) in (37) gives us that for $\forall x \in [a, b]$ and for $\forall t$,

$$\left|c\left(x + e^{\kappa \Delta t}\epsilon_1, t\right) - c(x, t)\right| \leqslant e^a e^{\kappa \Delta t}|\epsilon_1| =: \hat{\epsilon}_c,$$

which implies $|\epsilon_c(x, t_{M-1})| \leqslant \hat{\epsilon}_c$. Now we look at the error in the early-exercise point at t_{M-1}. Assume points $x^*_{t_{M-1}}$ and $x^*_{t_{M-1}} + \epsilon_x(t_{M-1})$ are the early-exercise points obtained from the original and the approximate characteristic functions, respectively. It follows that

$$\begin{aligned}
&c\left(x^*_{t_{M-1}}, t_{M-1}\right) = g\left(x^*_{t_{M-1}}, t_{M-1}\right),\\
&\hat{c}\left(x^*_{t_{M-1}} + \epsilon_x(t_{M-1}), t_{M-1}\right) = g\left(x^*_{t_{M-1}} + \epsilon_x(t_{M-1}), t_{M-1}\right).
\end{aligned}$$

Therefore

$$\begin{aligned}
&g\left(x^*_{t_{M-1}} + \epsilon_x(t_{M-1}), t_{M-1}\right) - c\left(x^*_{t_{M-1}} + \epsilon_x(t_{M-1}), t_{M-1}\right)\\
&\quad = \hat{c}\left(x^*_{t_{M-1}} + \epsilon_x(t_{M-1}), t_{M-1}\right) - c\left(x^*_{t_{M-1}} + \epsilon_x(t_{M-1}), t_{M-1}\right)\\
&\quad =: \epsilon_c\left(x^*_{t_{M-1}} + \epsilon_x(t_{M-1}), t_{M-1}\right).
\end{aligned}$$

[2] It is non-decreasing is because the payoff of a put option is convex, which implies that the gamma, $\partial c^2(x, t)/\partial x^2$, is non-negative indicating a non-decreasing first derivative $\partial c(x, t)/\partial x$. This holds for a long position in the option.

We introduce a new function $h(x,t) := g(x,t) - c(x,t)$, so that we have

$$h\big(x^*_{t_{M-1}}, t_{M-1}\big) = 0,$$
$$h\big(x^*_{t_{M-1}} + \epsilon_x(t_{M-1}), t_{M-1}\big) = \epsilon_c\big(x^*_{t_{M-1}} + \epsilon_x(t_{M-1}), t_{M-1}\big).$$

Application of (34) gives:

$$\big|h\big(x^*_{t_{M-1}} + \epsilon_x(t_{M-1}), t_{M-1}\big) - h\big(x^*_{t_{M-1}}, t_{M-1}\big)\big| = \big|\epsilon_c\big(x^*_{t_{M-1}} + \epsilon_x(t_{M-1}), t_{M-1}\big)\big| \leqslant \hat{\epsilon}_c. \tag{41}$$

Using Lagrange's mean value theorem for (41) gives us

$$\big|\epsilon_x(t_{M-1})\big|\big|h'(\bar{\delta}, t_{M-1})\big| \leqslant \hat{\epsilon}_c,$$

for some $\bar{\delta} \in (x^*_{t_{M-1}}, x^*_{t_{M-1}} + \epsilon_x(t_{M-1}))$.

The fact that there is one early-exercise point for plain Bermudan put options implies that

$$\big|h\big(x^*_{t_{M-1}} + \epsilon_x(t_{M-1}), t_{M-1}\big) - h\big(x^*_{t_{M-1}}, t_{M-1}\big)\big| > 0.$$

If there is an error in the early-exercise point, i.e. if $\epsilon_x(t_{M-1}) \neq 0$, we have that $|h'(\bar{\delta}, t_{M-1})| > 0$, so that

$$\big|\epsilon_x(t_{M-1})\big| \leqslant \frac{\hat{\epsilon}_c}{|h'(\bar{\delta}, t_{M-1})|}. \tag{42}$$

Hence $|\epsilon_x(t_{M-1})|$ is bounded in terms of $\hat{\epsilon}_c$. If $\hat{\epsilon}_c$ tends to zero, then $|\epsilon_x(t_{M-1})|$ also tends to zero. □

At the other time points, $m = 0, \ldots, M-2$, the upper bound for the shift in the early-exercise point can also be determined in terms of the error in the continuation value. However, unlike time step t_{M-1}, the error in the continuation value is not only related to the approximate characteristic function, but also to the error in $V_k(t)$,

$$V_k(t) := \int_a^b \max\big(c(x,t), g(x,t)\big) \cos\left(k\pi \frac{x-a}{b-a}\right) dx.$$

We first have a look at the error in $V_k(t_{M-1})$ from (15) in the following lemma. We will need the results in the lemma to derive upper bounds in the lemmas to follow.

Lemma 4.3. *For $\epsilon_x(t_{M-1}) > 0$, two points, $\delta_1 \in (x^*_{t_{M-1}} + \epsilon_x(t_{M-1}), b)$ and $\delta_2 \in (x^*_{t_{M-1}}, x^*_{t_{M-1}} + \epsilon_x(t_{M-1}))$ exist, so that*

$$\epsilon_V(t_{M-1}) = \epsilon_c(\delta_1, t_{M-1}) I_k\big(x^*_{t_{M-1}} + \epsilon_x(t_{M-1}), b\big) + \big(g(\delta_2, t_{M-1}) - c(\delta_2, t_{M-1})\big) I_k\big(x^*_{t_{M-1}}, x^*_{t_{M-1}} + \epsilon_x(t_{M-1})\big), \tag{43}$$

where

$$I_k(x_1, x_2) = \frac{2}{b-a} \int_{x_1}^{x_2} \cos\left(k\pi \frac{x-a}{b-a}\right) dx, \tag{44}$$

can be viewed as the (analytically available) Fourier-cosine coefficient of an option with value:

$$v_I(x, x_1, x_2) = \begin{cases} 1 & \text{if } x \in [x_1, x_2], \\ 0 & \text{otherwise.} \end{cases} \tag{45}$$

Moreover, we have that $|\epsilon_c(\delta_1, t_{M-1})| \leqslant \hat{\epsilon}_c$, and

$$\big|g(\delta_2, t_{M-1}) - c(\delta_2, t_{M-1})\big| \leqslant \hat{\epsilon}_c. \tag{46}$$

Proof. Here we assume that both early-exercise points, for the original and approximate OU processes, lie in the integration range. If either x^* or $x^* + \epsilon_x$ lies outside range $[a,b]$, it is set equal to the nearest boundary point. V_k can thus be split as in (15) depending on the early-exercise point.

Let us first analyze the case of a *positive error*, $\epsilon_x(t_{M-1})$, in the early-exercise point at t_{M-1}. Between $x^*_{t_{M-1}} + \epsilon_x(t_{M-1})$ and b, for the original and the approximate OU processes, we use the continuation value. The error in $V_k(t_{M-1})$ in this interval originates from the error in the continuation value, $\epsilon_c(x, t_{M-1})$. This error, which is denoted by $\epsilon_{V_1}(t_{M-1})$, reads:

$$\epsilon_{V_1}(t_{M-1}) = \frac{2}{b-a} \int_{x^*_{t_{M-1}} + \epsilon_x(t_{M-1})}^{b} \epsilon_c(x, t_{M-1}) \cos\left(k\pi \frac{x-a}{b-a}\right) dx.$$

By application of the first mean value theorem for integration, there exists a $\delta_1 \in (x^*_{t_{M-1}} + \epsilon_x(t_{M-1}), b)$, so that

$$\begin{aligned}\epsilon_{V_1}(t_{M-1}) &= \frac{2\epsilon_c(\delta_1, t_{M-1})}{b-a} \int_{x^*_{t_{M-1}}+\epsilon_x(t_{M-1})}^{b} \cos\left(k\pi \frac{x-a}{b-a}\right) dx \\ &= \epsilon_c(\delta_1, t_{M-1}) I_k\big(x^*_{t_{M-1}} + \epsilon_x(t_{M-1}), b\big), \end{aligned} \tag{47}$$

with I_k from (44). From (34) we have that $|\epsilon_c(\delta_1, t_{M-1})| \leqslant \hat{\epsilon}_c$.

Between a and $x^*_{t_{M-1}}$, for both the original and approximate OU processes, we take the payoff function which for a put option reads $g(x,t) = \max(K - e^x, 0)$. There is no error in the payoff function, hence no error in $V_k(t_{M-1})$ along this part of the x-axis.

Between $x^*_{t_{M-1}}$ and $x^*_{t_{M-1}} + \epsilon_x(t_{M-1})$, with the original OU process we use continuation value, $c(x, t_{M-1})$. However, due to the shift in the early-exercise point we have the payoff $g(x, t_{M-1})$ instead when using the approximate OU process. This leads to an error in $V_k(t_{M-1})$, denoted by $\epsilon_{V_2}(t_{M-1})$, which reads:

$$\epsilon_{V_2}(t_{M-1}) = \frac{2}{b-a} \int_{x^*_{t_{M-1}}}^{x^*_{t_{M-1}}+\epsilon_x(t_{M-1})} \big(g(x, t_{M-1}) - c(x, t_{M-1})\big) \cos\left(k\pi \frac{x-a}{b-a}\right) dx.$$

By application again of the first mean value theorem for integration, there exists a $\delta_2 \in (x^*_{t_{M-1}}, x^*_{t_{M-1}} + \epsilon_x(t_{M-1}))$, so that

$$\begin{aligned}\epsilon_{V_2}(t_{M-1}) &= \big(g(\delta_2, t_{M-1}) - c(\delta_2, t_{M-1})\big) \cdot \frac{2}{b-a} \int_{x^*_{t_{M-1}}}^{x^*_{t_{M-1}}+\epsilon_x(t_{M-1})} \cos\left(k\pi \frac{x-a}{b-a}\right) dx \\ &= \big(g(\delta_2, t_{M-1}) - c(\delta_2, t_{M-1})\big) I_k\big(x^*_{t_{M-1}}, x^*_{t_{M-1}} + \epsilon_x(t_{M-1})\big). \end{aligned} \tag{48}$$

For a put option, $\forall t$, for all $x > x^*_t$, $c(x,t) - g(x,t) > 0$, and function $c(x,t) - g(x,t)$ is non-decreasing[3] between x^*_t and $x^*_t + \epsilon_x(t)$. This implies:

$$\begin{aligned}\big|g(\delta_2, t_{M-1}) - c(\delta_2, t_{M-1})\big| &= c(\delta_2, t_{M-1}) - g(\delta_2, t_{M-1}) \\ &\leqslant c\big(x^*_{t_{M-1}} + \epsilon_x(t_{M-1}), t_{M-1}\big) - g\big(x^*_{t_{M-1}} + \epsilon_x(t_{M-1}), t_{M-1}\big) \\ &= \big|\epsilon_c\big(x^*_{t_{M-1}} + \epsilon_x(t_{M-1}), t_{M-1}\big)\big| \\ &\leqslant \hat{\epsilon}_c. \end{aligned}$$

The last step is from (34).

Adding up (47) and (48) gives

$$\begin{aligned}\epsilon_V(t_{M-1}) &= \epsilon_{V_1}(t_{M-1}) + \epsilon_{V_2}(t_{M-1}) \\ &= \epsilon_c(\delta_1, t_{M-1}) I_k\big(x^*_{t_{M-1}} + \epsilon_x(t_{M-1}), b\big) + \big(g(\delta_2, t_{M-1}) - c(\delta_2, t_{M-1})\big) I_k\big(x^*_{t_{M-1}}, x^*_{t_{M-1}} + \epsilon_x(t_{M-1})\big). \end{aligned}$$ □

Remark 4.1. The case when $\epsilon_x(t_{M-1}) < 0$ goes similarly. It can then be proved that points $\delta_1 \in (x^*_{t_{M-1}}, b)$ and $\delta_2 \in (x^*_{t_{M-1}} + \epsilon_x(t_{M-1}), x^*_{t_{M-1}})$ exist, so that

$$\epsilon_V(t_{M-1}) = \epsilon_c(\delta_1, t_{M-1}) I_k\big(x^*_{t_{M-1}}, b\big) + \big(\hat{c}(\delta_2, t_{M-1}) - g(\delta_2, t_{M-1})\big) I_k\big(x^*_{t_{M-1}} + \epsilon_x(t_{M-1}), x^*_{t_{M-1}}\big). \tag{49}$$

Moreover, $|\epsilon_c(\delta_1, t_{M-1})| \leqslant \hat{\epsilon}_c$, and $|\hat{c}(\delta_2, t_{M-1}) - g(\delta_2, t_{M-1})| \leqslant \hat{\epsilon}_c$.

4.2. Further steps in the backward recursion

We analyze the case $t = t_{M-2}$ in the following lemma.

Lemma 4.4. *For* $\forall x \in [a,b]$, $|\epsilon_c(x, t_{M-2})| \leqslant \hat{\epsilon}_c(1 + e^{-r\Delta t})$.

[3] For put options in log-scale when $x \leqslant 0$, function $c(x,t) - g(x,t)$ is non-decreasing and for $x \geqslant 0$, $c(x,t) - g(x,t)$ is non-increasing. For a put option early-exercise points are negative. Therefore, between the two early-exercise points, x^*_t and $x^*_t + \epsilon_x(t)$, $c(x,t) - g(x,t)$ is non-decreasing.

Proof. At $t = t_{M-2}$ we have

$$\begin{aligned}\left|\epsilon_c(x,t_{M-2})\right| &:= \left|\hat{c}(x,t_{M-2}) - c(x,t_{M-2})\right| \\ &= \left| e^{-r\Delta t} \sum_{k=0}^{N-1}{}' \operatorname{Re}\left(\phi_{app}\left(\frac{k\pi}{b-a}; x, \Delta t\right) e^{-ik\pi\frac{a}{b-a}}\right)\left(V_k(t_{M-1}) + \epsilon_V(t_{M-1})\right)\right. \\ &\quad \left. - e^{-r\Delta t} \sum_{k=0}^{N-1}{}' \operatorname{Re}\left(\phi_{ou}\left(\frac{k\pi}{b-a}; x, \Delta t\right) e^{-ik\pi\frac{a}{b-a}}\right) V_k(t_{M-1})\right|. \end{aligned} \tag{50}$$

Application of (32) gives:

$$\begin{aligned}\left|\epsilon_c(x,t_{M-2})\right| &\leqslant \left| e^{-r\Delta t} \sum_{k=0}^{N-1}{}' \operatorname{Re}\left(\phi_{app}\left(\frac{k\pi}{b-a}; x, \Delta t\right) e^{-ik\pi\frac{a}{b-a}}\right)\epsilon_V(t_{M-1})\right| \\ &\quad + \left| e^{-r\Delta t} \sum_{k=0}^{N-1}{}' \operatorname{Re}\left(\phi_{ou}\left(\frac{k\pi}{b-a}; x + e^{\kappa\Delta t}\epsilon_1, \Delta t\right) e^{-ik\pi\frac{a}{b-a}}\right) V_k(t_{M-1})\right. \\ &\quad \left. - e^{-r\Delta t} \sum_{k=0}^{N-1}{}' \operatorname{Re}\left(\phi_{ou}\left(\frac{k\pi}{b-a}; x, \Delta t\right) e^{-ik\pi\frac{a}{b-a}}\right) V_k(t_{M-1})\right| \\ &\leqslant \left| e^{-r\Delta t} \sum_{k=0}^{N-1}{}' \operatorname{Re}\left(\phi_{app}\left(\frac{k\pi}{b-a}; x, \Delta t\right) e^{-ik\pi\frac{a}{b-a}}\right)\epsilon_V(t_{M-1})\right| + \hat{\epsilon}_c. \end{aligned} \tag{51}$$

The last step is from (33).

By application of Lemma 4.3, Eq. (46) we have that, for $\epsilon_x(t_{M-1}) > 0$,

$$\begin{aligned}&\left| e^{-r\Delta t} \sum_{k=0}^{N-1}{}' \operatorname{Re}\left(\phi_{app}\left(\frac{k\pi}{b-a}; x, \Delta t\right) e^{-ik\pi\frac{a}{b-a}}\right)\epsilon_V(t_{M-1})\right| \\ &\leqslant \left|\epsilon_c(\delta_1, t_{M-1})\right| \cdot \left| e^{-r\Delta t} \sum_{k=0}^{N-1}{}' \operatorname{Re}\left(\phi_{app}\left(\frac{k\pi}{b-a}; x, \Delta t\right) e^{-ik\pi\frac{a}{b-a}}\right) I_k\left(x^*_{t_{M-1}} + \epsilon_x(t_{M-1}), b\right)\right| \\ &\quad + \left|g(\delta_2, t_{M-1}) - c(\delta_2, t_{M-1})\right| \cdot \left| e^{-r\Delta t} \sum_{k=0}^{N-1}{}' \operatorname{Re}\left(\phi_{app}\left(\frac{k\pi}{b-a}; x, \Delta t\right) e^{-ik\pi\frac{a}{b-a}}\right) I_k\left(x^*_{t_{M-1}}, x^*_{t_{M-1}} + \epsilon_x(t_{M-1})\right)\right| \\ &\leqslant \hat{\epsilon}_c e^{-r\Delta t} \sum_{k=0}^{N-1}{}' \operatorname{Re}\left(\phi_{app}\left(\frac{k\pi}{b-a}; x, \Delta t\right) e^{-ik\pi\frac{a}{b-a}}\right)\left(I_k\left(x^*_{t_{M-1}} + \epsilon_x(t_{M-1}), b\right) + I_k\left(x^*_{t_{M-1}}, x^*_{t_{M-1}} + \epsilon_x(t_{M-1})\right)\right) \\ &= \hat{\epsilon}_c v_I\left(x + e^{\kappa\Delta t}\epsilon_1, x^*_{t_{M-1}}, b\right), \end{aligned} \tag{52}$$

where we have used the fact that option values, represented by the cosine series with $I_k(\cdot,\cdot)$, are positive. From (45) we have

$$\begin{aligned} v_I\left(x + e^{\kappa\Delta t}\epsilon_1, x^*_{t_{M-1}}, b\right) &= e^{-r\Delta t} \int_{\mathbb{R}} f\left(y | x + e^{\kappa\Delta t}\epsilon_1, \Delta t\right) I(y)\, dy \\ &\leqslant e^{-r\Delta t} \int_{\mathbb{R}} f\left(y | x + e^{\kappa\Delta t}\epsilon_1, \Delta t\right) dy = e^{-r\Delta t}. \end{aligned} \tag{53}$$

Substitution of (53) in (52) gives us

$$\left| e^{-r\Delta t} \sum_{k=0}^{N-1}{}' \operatorname{Re}\left(\phi_{app}\left(\frac{k\pi}{b-a}; x, \Delta t\right) e^{-ik\pi\frac{a}{b-a}}\right)\epsilon_V(t_{M-1})\right| \leqslant \hat{\epsilon}_c e^{-r\Delta t}. \tag{54}$$

By using (54) in (51), we obtain

$$\left|\epsilon_c(x,t_{M-2})\right| \leqslant \hat{\epsilon}_c + \hat{\epsilon}_c e^{-r\Delta t} = \hat{\epsilon}_c\left(1 + e^{-r\Delta t}\right).$$

When $\epsilon_x(t_{M-1}) < 0$ it follows similarly, from (51) and Remark 4.1, that

$$\begin{aligned}\left|\epsilon_c(x,t_{M-2})\right| &\leqslant \hat{\epsilon}_c + \left|e^{-r\Delta t}\sum_{k=0}^{N-1}{}'\,\mathrm{Re}\left(\phi_{app}\left(\frac{k\pi}{b-a};x,\Delta t\right)e^{-ik\pi\frac{a}{b-a}}\right)\epsilon_V(t_{M-1})\right| \\ &\leqslant \hat{\epsilon}_c + \left|\epsilon_c(\delta_1,t_{M-1})\right|\cdot\left|v_I\left(x+e^{\kappa\Delta t}\epsilon_1,x^*_{t_{M-1}},b\right)\right| \\ &\quad + \left|\hat{c}(\delta_2,t_{M-1})-g(\delta_2,t_{M-1})\right|\cdot\left|v_I\left(x+e^{\kappa\Delta t}\epsilon_1,x^*_{t_{M-1}}+\epsilon_x(t_{M-1}),x^*_{t_{M-1}}\right)\right| \\ &\leqslant \hat{\epsilon}_c\left(1+e^{-r\Delta t}\right). \qquad \square\end{aligned} \tag{55}$$

The relations in (34) and Lemma 4.4 serve as the first steps in a mathematical induction proof to find an upper bound for $\epsilon_c(t_0)$, the error in the Bermudan option price at t_0, as follows:

Theorem 4.1. *For $\forall\, x\in[a,b]$, $j\in\{1,\ldots,M-1\}$, we assume that*

$$\epsilon_c(x,t_{M-j}) \leqslant \hat{\epsilon}_c\sum_{l=1}^{j}e^{-r(l-1)\Delta t}. \tag{56}$$

Then, it follows that, $\forall x$,

$$\epsilon_c(x,t_{M-(j+1)}) \leqslant \hat{\epsilon}_c\sum_{l=1}^{j+1}e^{-r(l-1)\Delta t}. \tag{57}$$

Proof. At $t_{M-(j+1)}$, we have

$$\begin{aligned}\left|\epsilon_c(x,t_{M-(j+1)})\right| &= \left|\hat{c}(x,t_{M-(j+1)})-c(x,t_{M-(j+1)})\right| \\ &= \left|e^{-r\Delta t}\sum_{k=0}^{N-1}{}'\,\mathrm{Re}\left(\phi_{app}\left(\frac{k\pi}{b-a};x,\Delta t\right)e^{-ik\pi\frac{a}{b-a}}\right)\left(V_k(t_{M-j})+\epsilon_V(t_{M-j})\right)\right. \\ &\quad \left. - e^{-r\Delta t}\sum_{k=0}^{N-1}{}'\,\mathrm{Re}\left(\phi_{ou}\left(\frac{k\pi}{b-a};x,\Delta t\right)e^{-ik\pi\frac{a}{b-a}}\right)V_k(t_{M-j})\right| \\ &\leqslant \left|e^{-r\Delta t}\sum_{k=0}^{N-1}{}'\,\mathrm{Re}\left(\phi_{app}\left(\frac{k\pi}{b-a};x,\Delta t\right)e^{-ik\pi\frac{a}{b-a}}\right)\epsilon_V(t_{M-j})\right| + \hat{\epsilon}_c,\end{aligned} \tag{58}$$

where the last step follows from (33).

With arguments as in Lemma 4.3 and its proof, we have that for $\epsilon_x(t_{M-j})>0$, values $\delta_1\in(x^*_{t_{M-j}}+\epsilon_x(t_{M-j}),b)$ and $\delta_2\in(x^*_{t_{M-j}},x^*_{t_{M-j}}+\epsilon_x(t_{M-j}))$ exist, so that,

$$\epsilon_V(t_{M-j}) = \epsilon_c(\delta_1,t_{M-j})I_k\left(x^*_{t_{M-j}}+\epsilon_x(t_{M-j}),b\right)+\left(g(\delta_2,t_{M-j})-c(\delta_2,t_{M-j})\right)I_k\left(x^*_{t_{M-j}},x^*_{t_{M-j}}+\epsilon_x(t_{M-j})\right).$$

With the induction assumptions:

$$\left|\epsilon_c(\delta_1,t_{M-j})\right| \leqslant \hat{\epsilon}_c\sum_{l=1}^{j}e^{-r(l-1)\Delta t}, \tag{59}$$

and

$$\left|g(\delta_2,t_{M-j})-c(\delta_2,t_{M-j})\right| \leqslant \left|\epsilon_c\left(x^*_{t_{M-j}}+\epsilon_x(t_{M-j}),t_{M-j}\right)\right| \leqslant \hat{\epsilon}_c\sum_{l=1}^{j}e^{-r(l-1)\Delta t}, \tag{60}$$

and by similar arguments as in Lemma 4.4 and its proof, we have that for positive errors in the early-exercise point at t_{M-j},

$$\left|e^{-r\Delta t}\sum_{k=0}^{N-1}{}'\,\mathrm{Re}\left(\phi_{app}\left(\frac{k\pi}{b-a};x,\Delta t\right)e^{-ik\pi\frac{a}{b-a}}\right)\epsilon_V(t_{M-j})\right|$$

$$\leqslant \hat{\epsilon}_c \sum_{l=1}^{j} e^{-r(l-1)\Delta t} v_I\big(x + e^{\kappa\Delta t}\epsilon_1, \min\big(x^*_{t_{M-j}}, x^*_{t_{M-j}} + \epsilon_x(t_{M-j})\big), b\big)$$

$$\leqslant \hat{\epsilon}_c \sum_{l=1}^{j} e^{-r(l-1)\Delta t} e^{-r\Delta t} = \hat{\epsilon}_c \sum_{l=2}^{j+1} e^{-r(l-1)\Delta t}. \tag{61}$$

Therefore, we find that, for $\forall x \in [a,b]$:

$$\big|\epsilon_c(x, t_{M-(j+1)})\big| \leqslant \hat{\epsilon}_c \sum_{l=2}^{j+1} e^{-r(l-1)\Delta t} + \hat{\epsilon}_c = \hat{\epsilon}_c \sum_{l=1}^{j+1} e^{-r(l-1)\Delta t}. \qquad \square \tag{62}$$

Remark 4.2. When $\epsilon_x(t_{M-j}) < 0$, the proof goes similarly, and we can find that $\delta_1 \in (x^*_{t_{M-j}}, b)$ and $\delta_2 \in (x^*_{t_{M-j}} + \epsilon_x(t_{M-j}), x^*_{t_{M-j}})$ exist, so that

$$\epsilon_V(t_{M-j}) = \epsilon_c(\delta_1, t_{M-j}) I_k\big(x^*_{t_{M-j}}, b\big) + \big(\hat{c}(\delta_2, t_{M-j}) - g(\delta_2, t_{M-j})\big) I_k\big(x^*_{t_{M-j}} + \epsilon_x(t_{M-j}), x^*_{t_{M-j}}\big).$$

With the induction assumptions,

$$\big|\epsilon_c(\delta_1, t_{M-j})\big| \leqslant \hat{\epsilon}_c \sum_{l=1}^{j} e^{-r(l-1)\Delta t},$$

and

$$\big|\hat{c}(\delta_2, t_{M-j}) - g(\delta_2, t_{M-j})\big| \leqslant \big|\epsilon_c\big(x^*_{t_{M-j}}, t_{M-j}\big)\big| \leqslant \hat{\epsilon}_c \sum_{l=1}^{j} e^{-r(l-1)\Delta t},$$

we can then also prove the inequalities (61) and (62) to hold.

It follows directly from (34), Lemma 4.4 and Theorem 4.1 that at t_0, for any x, the error in the Bermudan option price satisfies:

$$\big|\epsilon_c(x, t_0)\big| \leqslant \hat{\epsilon}_c \sum_{l=1}^{M} e^{-r(l-1)\Delta t} = \hat{\epsilon}_c \frac{1 - e^{-rT}}{1 - e^{-r\Delta t}} = |\epsilon_1| e^{\kappa\Delta t} e^{a} \frac{1 - e^{-rT}}{1 - e^{-r\Delta t}}.$$

To obtain accuracy up to one basis point[4] for Bermudan options, with the approximate OU process, we prescribe that for all x,

$$\big|\epsilon_c(x, t_0)\big| < 4 \cdot 10^{-5},$$

which is equivalent to

$$|\epsilon_1| < e^{-\kappa\Delta t} e^{-a} \frac{1 - e^{-r\Delta t}}{1 - e^{-rT}} \cdot 4 \cdot 10^{-5}.$$

Therefore, the approximate characteristic function (28) and thus the Fast Fourier Transform can be applied for pricing Bermudan options, if

$$|\epsilon_1| := \big|x - \mathbb{E}(x)\big|\big(1 - e^{-\kappa\Delta t}\big) < e^{-\kappa\Delta t} e^{-a} \frac{1 - e^{-r\Delta t}}{1 - e^{-rT}} \cdot 4 \cdot 10^{-5} =: TOL. \tag{63}$$

Finally, we need an approximation for $|\epsilon_1|$ in practice. Note that

$$0 \leqslant \big(\mathbb{E}\big|\big(x - \mathbb{E}(x)\big)\big|\big)^2 \leqslant \mathbb{E}\big|x - \mathbb{E}(x)\big|^2 = \mathbb{V}\mathrm{ar}(x) \leqslant \frac{\sigma^2}{2\kappa}.$$

So,

$$\mathbb{E}\big(\big|x - \mathbb{E}(x)\big|\big) \leqslant \frac{\sigma}{\sqrt{2\kappa}}. \tag{64}$$

In our implementation we use the upper bound of this expected value to estimate $|\epsilon_1|$ and apply the Fast Fourier Transform with the approximate characteristic function if $\frac{\sigma}{\sqrt{2\kappa}}(1 - e^{-\kappa\Delta t})$ is below the tolerance level defined by (63).

[4] To ensure the basis point precision the error in the option price should be less than 10^{-4}. We also consider the influence of rounding up errors, and set therefore $4 \cdot 10^{-5}$ here.

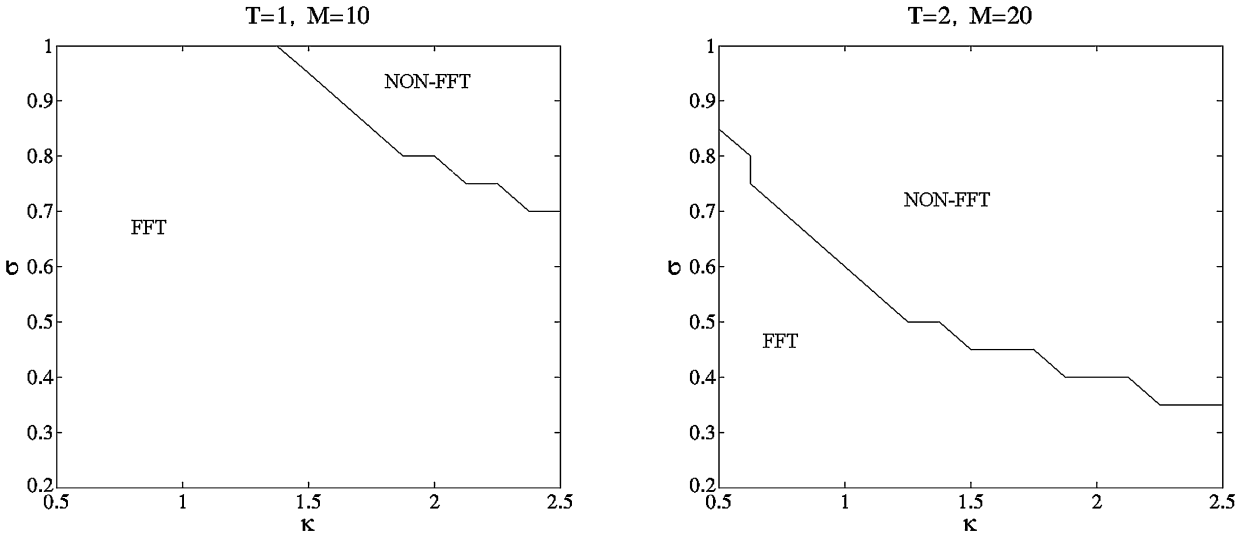

(a) $T = 1, M = 10$ (b) $T = 2, M = 20$

Fig. 1. FFT and non-FFT parameter ranges for different maturities, with $\Delta t = 0.1$.

5. Numerical results

The FFT can be applied in the parameter range for which

$$\hat{\epsilon}_1 := \frac{\sigma}{\sqrt{2\kappa}}\left(1 - e^{-\kappa \Delta t}\right) < TOL,$$

with tolerance level *TOL* defined in (63). In the so-called "non-FFT range", where $\hat{\epsilon}_1 > TOL$, we use the characteristic function of the original OU process to ensure accurate Bermudan option prices.

MATLAB 7.7.0 has been used for all numerical experiments and the CPU is an Intel(R) Core(TM)2 Duo CPU E6550 (@ 2.33 GHz Cache size 4 MB). CPU time is recorded in seconds.

Fig. 1 compares the FFT ranges with a fixed Δt, but with different maturities, T. With Δt fixed, $\hat{\epsilon}_1$ remains the same for the same κ and σ for all maturities. However, as T increases, the tolerance level (63) decreases so that we find a tighter criterion regarding the use of the FFT.

As σ (y-axis in Fig. 1) increases to certain values, we cannot employ the approximate OU model anymore, as $\hat{\epsilon}_1$ increases, resulting in a large error in the Bermudan option price.

An increase in parameter κ (x-axis in Fig. 1) also leads to a decrease of the size of the FFT range, see Fig. 1, due to an increase in the value of $\hat{\epsilon}_1$ and a reduction in the tolerance level (63), see Fig. 2, where $\hat{\epsilon}_1 - TOL$ is plotted as a function of κ.

Fig. 3 then presents the FFT and non-FFT ranges, with $M = 5$ and $M = 50$ for $T = 1$.

As parameter M, the number of exercise dates, increases, the range in which the FFT can be applied expands. However, the influence of M on the error and the tolerance level (63) is different for small and large model parameters. This is illustrated in Fig. 4. For small κ and σ (example in Fig. 4(a)), $\hat{\epsilon_1} - TOL$ is an increasing function of M, whereas for large model parameters (see Fig. 4(b)), $\hat{\epsilon_1} - TOL$ decreases as M increases.

This can be detailed by the derivative of $\hat{\epsilon_1} - TOL$ over M (in Fig. 5). In both cases, the quantity goes to zero as M increases, which implies that function $\hat{\epsilon_1} - TOL$ converges. For small parameters, $\hat{\epsilon_1} - TOL$ converges fast, so that these sets fall in the FFT range (see Fig. 3). On the other hand, as Fig. 5(b) shows, with large model parameters, $\hat{\epsilon_1} - TOL > 0$ when M is small. For large parameter values, the approximate model can thus be used for large values of M. This insight is particularly helpful for parameter sets at boundary of the FFT and non-FFT ranges which will be illustrated in the next subsection.

In our next tests we randomly choose different model parameters and check whether the numerical experiments are in accordance with our error analysis. The range of parameters is $\kappa \in [0.5, 2.5]$, $\sigma \in [0.2, 0.8]$, $M \in \{5, , \ldots, 20\}$, $T \in [1, 2]$, and we use seasonality function $G(t) = a_1 + a_2 \sin(a_3 t)$ with $a_1 = 3, 5, 10$, $a_2 \in [0.5, 2]$ and $a_3 \in [0.5, 2]$. Fig. 6(a) presents results for the OU process without seasonality, whereas Fig. 6(b) shows results for the approximate OU process with seasonality. The x-axes in the figures represent the logarithms of the error in the Bermudan option price.

In these numerical simulations we only consider the continuation values for the Bermudan options, as there is no error in the payoff function $g(x, t)$ neither in its Fourier-cosine coefficients G_k. For all parameter sets considered, the error is of order 10^{-4} or less, which implies that our approximation is accurate up to one basis point.

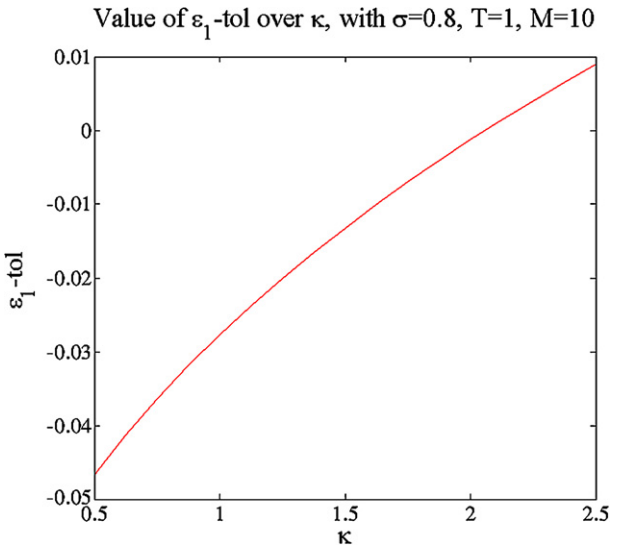

Fig. 2. Value of $\hat{\epsilon_1} - TOL$ over κ, with $T = 1$, $M = 10$, $\sigma = 0.8$.

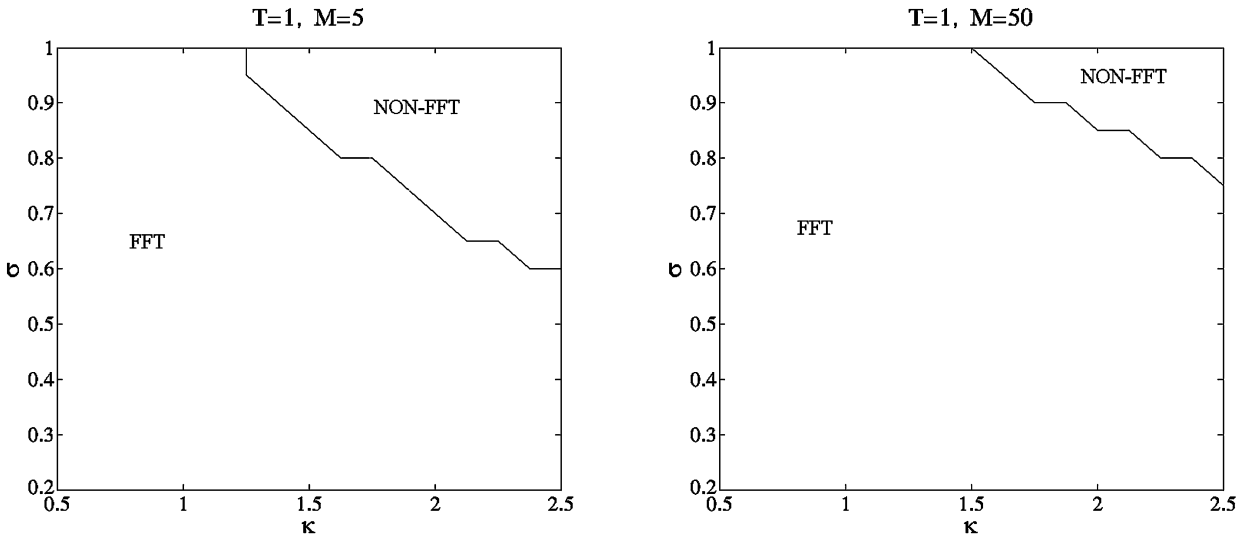

(a) $M = 5$ (b) $M = 50$

Fig. 3. FFT and non-FFT parameter ranges for different numbers of early-exercise dates, with $T = 1$.

5.1. CPU time and accuracy

We perform some more experiments checking the validity of the error analysis.

We first consider the OU process without seasonality and choose the following four sets of model parameters for the numerical examples and set $T = 1$ and $M = 10, 20, 50$:

1. $\kappa = 0.301$, $\sigma = 0.334$. This parameter set originates from commodity price calibration in [7].
2. $\kappa = 1$, $\sigma = 0.5$. This parameter set lies "in the FFT range" for $M = 10, 20, 50$, as in Fig. 3.
3. $\kappa = 2$, $\sigma = 0.7$. This parameter set is at the boundary of the FFT range (but still inside the FFT range) for $M = 10, 20, 50$, see Fig. 3.
4. $\kappa = 2.5$, $\sigma = 1$. This parameter set lies outside the FFT parameter range for $M = 10, 20, 50$, see Fig. 3.

For each parameter set, the CPU time, in seconds, as well as the error are recorded. We set $N = 512$ for which we are sure that convergence is achieved in space when $M = 20$ and $M = 50$.

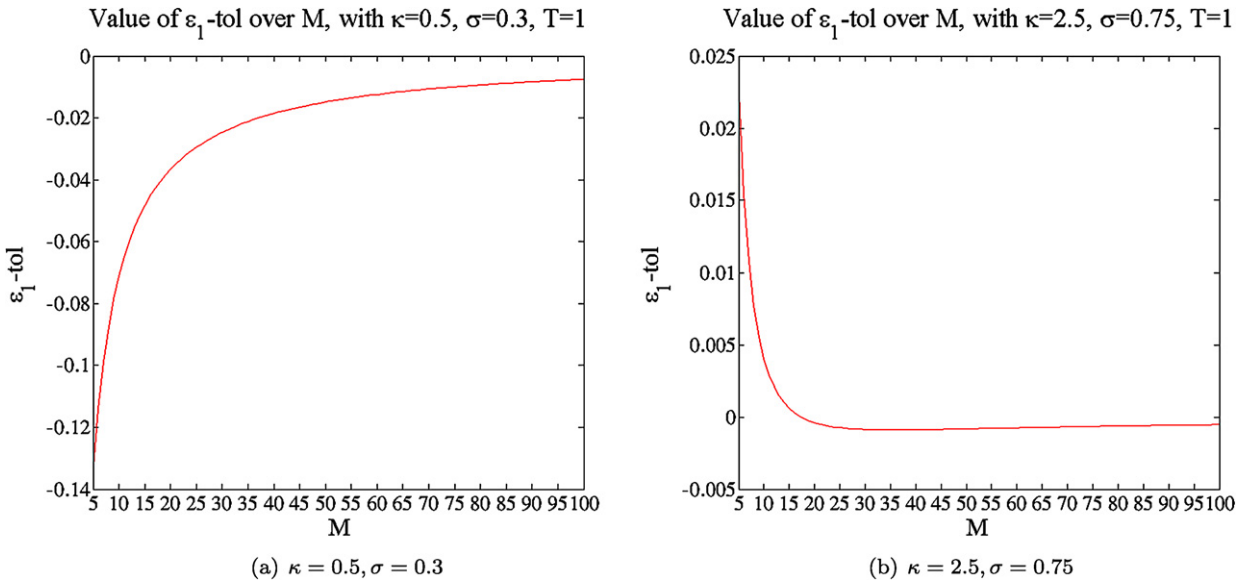

(a) $\kappa = 0.5, \sigma = 0.3$ (b) $\kappa = 2.5, \sigma = 0.75$

Fig. 4. Value of $\hat{\epsilon_1} - TOL$ over M, with (a) small value of κ and σ and (b) large value of κ and σ.

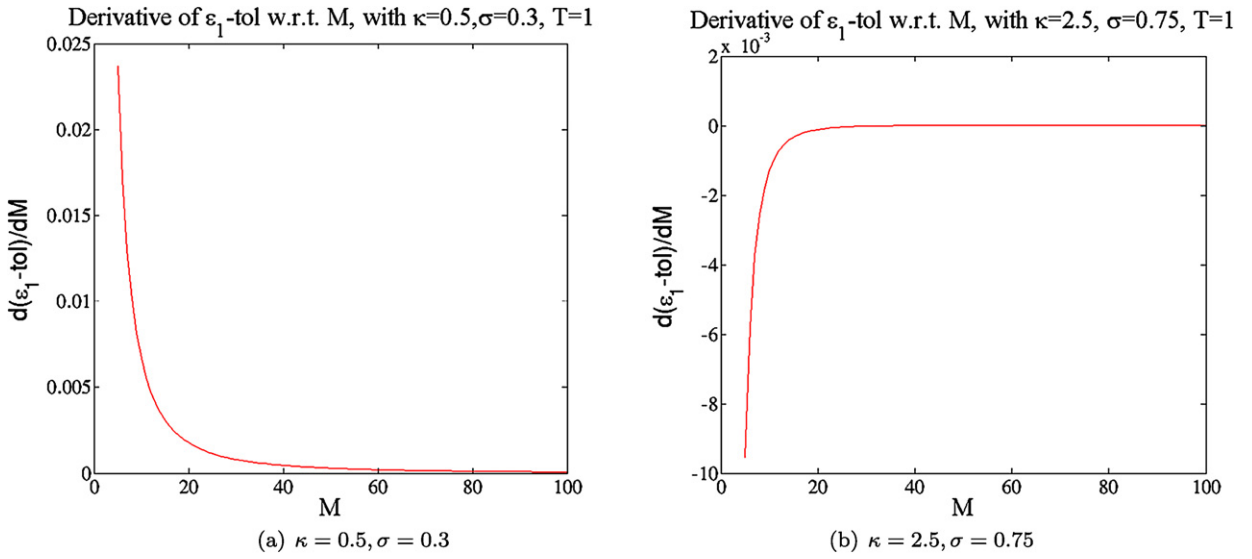

(a) $\kappa = 0.5, \sigma = 0.3$ (b) $\kappa = 2.5, \sigma = 0.75$

Fig. 5. Derivative of $\hat{\epsilon_1} - TOL$ with respective to M.

The numerical results are listed in Table 1, where *CPU time 1* and *CPU time 2* are the run-times of the Bermudan COS method with the original and the approximate OU model, respectively.[5] Moreover, the $\log_{10}$ (*error*) quantity in the table represents the logarithm of the absolute error in the Bermudan option price from the approximate model.

In Table 1 it is shown that for all parameter sets in the FFT range (sets 1 to 3), we can confirm the basis point precision. Moreover, the CPU time drops from seconds to milli-seconds if the FFT can be applied. As κ and σ increase (from sets 1 to 4), the error increases and the size of the FFT range reduces. This agrees with our analysis. For parameter set 4, for instance, only the use of the original characteristic function ensures the basis point precision.

Table 2 gives the results of the Delta value, the first derivative of the Bermudan option value with respect of the underlying stock price at $t = 0$. Here parameter sets 1–3 in the FFT range are used. From Table 2 we see that for these parameters, where according to our error analysis the approximation can be used, also the Delta value is within basis point precision.

[5] The FFT is used with the approximate OU model.

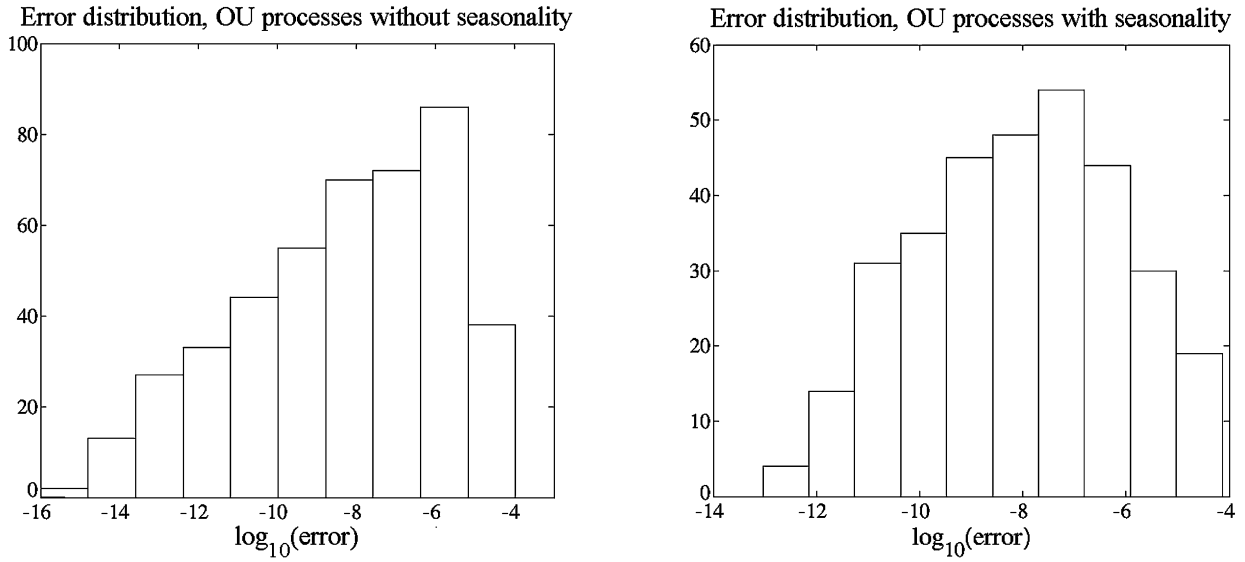

(a) Without Seasonality (b) With Seasonality

Fig. 6. Simulation result for OU processes: (a) without seasonality and (b) with seasonality.

Table 1
CPU time and error for the two OU processes and different model parameters.

	Parameter	Set 1	Set 2	Set 3	Set 4
$M = 10$	$\log_{10}$ (error)	−10.7784	−7.3434	−4.9392	−2.3424
	CPU time 1	15.2889	15.2108	15.2691	16.9608
	CPU time 2	0.0063	0.0064	0.0065	0.0064
$M = 20$	$\log_{10}$ (error)	−10.9893	−7.0835	−4.4139	−1.9757
	CPU time 1	31.8807	32.2614	32.3253	35.6780
	CPU time 2	0.0120	0.0122	0.0124	0.0124
$M = 50$	$\log_{10}$ (error)	−11.2600	−6.9289	−4.1043	−1.7612
	CPU time 1	81.9564	82.8565	91.6191	91.6244
	CPU time 2	0.0287	0.0296	0.0301	0.0300

Table 2
CPU time and error for the two OU processes and different model parameters.

	Parameter	Set 1	Set 2	Set 3
$M = 10$	$\log_{10}$ (error)	−10.4071	−7.2635	−5.1049
	CPU time 1	16.1995	15.5985	15.6600
	CPU time 2	0.0065	0.0065	0.0066
$M = 20$	$\log_{10}$ (error)	−10.6045	−6.9894	−4.5673
	CPU time 1	32.8128	33.1084	32.8150
	CPU time 2	0.0122	0.0125	0.0126
$M = 50$	$\log_{10}$ (error)	−10.4156	−6.8262	−4.2511
	CPU time 1	85.3691	84.5079	84.5922
	CPU time 2	0.0291	0.0301	0.0306

5.1.1. Probability density function of ϵ_1

In this subsection we take a closer look at the error in the characteristic function, ϵ_1:

$$\phi_{app}(u; x, \Delta t) = \phi_{ou}(u; x, \Delta t)e^{iu\epsilon_1}. \tag{65}$$

We have already seen that $\epsilon_1 := (x - \mathbb{E}(x))(1 - e^{-\kappa \Delta t})$. It is a normally distributed process, with $\mathbb{E}(\epsilon_1) = 0$ and $\mathbf{V}ar(\epsilon_1) = \frac{\sigma^2}{2\kappa}(1 - e^{-2\kappa t})(1 - e^{-\kappa \Delta t})$, because the OU process is also normally distributed.

Larger values of parameter t will give rise to larger variance in ϵ_1, with fixed value for Δt. Therefore we analyze here the error ϵ_1 at time point $T - \Delta t$, which gives us the largest variance in the backward recursion. The probability density functions for ϵ_1 with $T = 1$ and $T = 2$ are shown in Figs. 7 and 8, respectively. We have chosen the parameter sets used earlier, i.e., parameter set 1 with $\kappa = 0.301$ and $\sigma = 0.334$ (well in the FFT range) and set 3 with $\kappa = 2$ and $\sigma = 0.7$ (at the boundary of the FFT range) with $T = 1$. For $T = 2$ we used $\sigma = 0.4$ in set 3, so that this set also falls in the FFT range for this test.

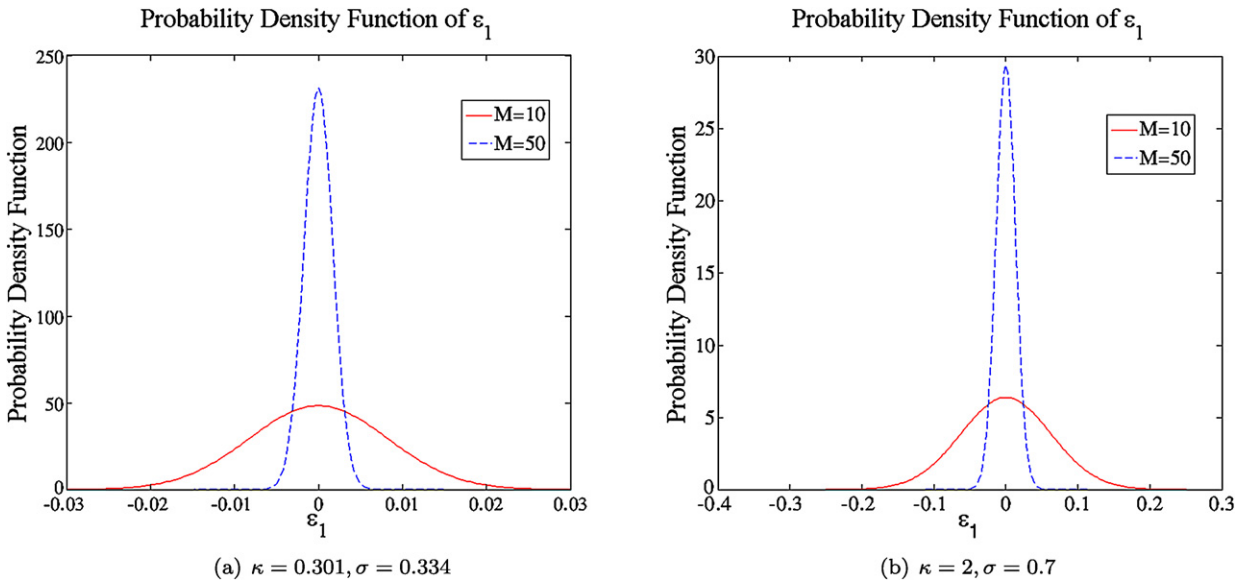

Fig. 7. Probability density function of ϵ_1 with $T = 1$.

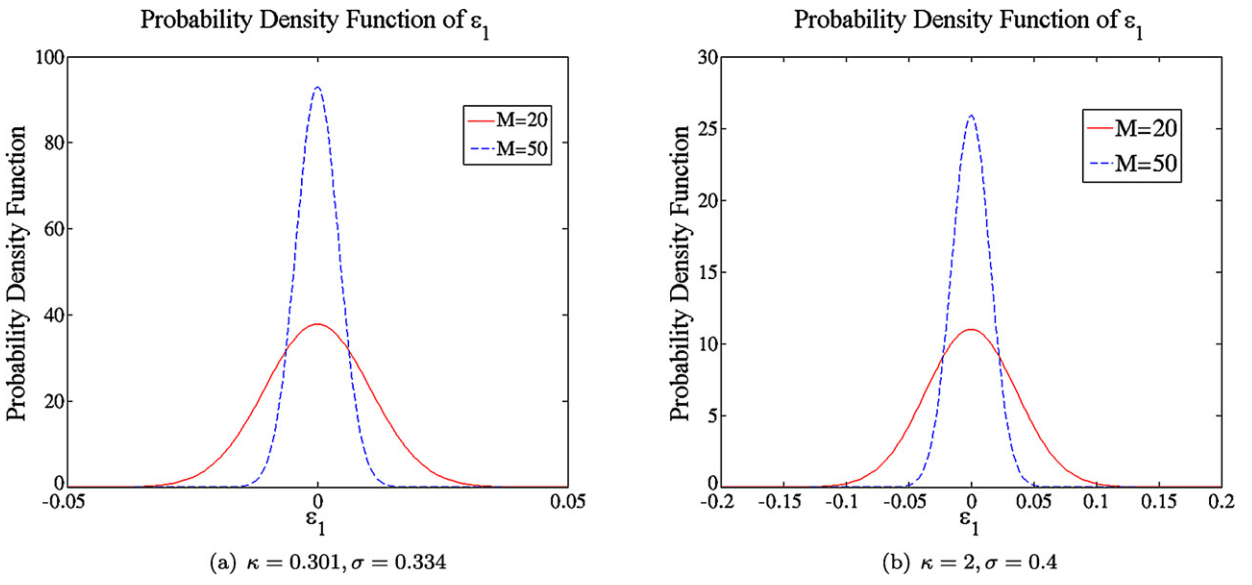

Fig. 8. Probability density function of ϵ_1 with $T = 2$.

For the OU processes with and without seasonality, when model parameters are fixed, the density function of ϵ_1 is essentially the same (with the same variance).

From Figs. 7 and 8 we see that with T fixed, larger values for M result in smaller errors in ϵ_1. Moreover, small values for κ and σ also bring smaller errors in characteristic function, compared to the larger model parameters.

5.1.2. Early-exercise points

In this subsection we compare the early-exercise points obtained from the original and approximate characteristic functions, $\phi_{ou}(u; x, \Delta t)$ and $\phi_{app}(u; x, \Delta t)$, respectively. We present early-exercise point $x^*_{t=\Delta t}$, i.e. the value at the last time step of the backward recursion, with $T = 1$ and $M = 10, 20, 50$.

We use here parameter set 1 ($\kappa = 0.301$, $\sigma = 0.334$) and parameter set 3 ($\kappa = 2$, $\sigma = 0.7$, at the boundary of the FFT parameter range).

The results are shown in Table 3.

Table 3
Early-exercise points at $t = \Delta t$ for Bermudan put options; parameter sets 1 and 3, $T = 1$, different values for M (no seasonality).

M	$M = 10$	$M = 20$	$M = 50$
Set 1, $\phi_{ou}(u; x, \Delta t)$	3.1438	3.1489	3.1516
Set 1, $\phi_{app}(u; x, \Delta t)$	3.1277	3.0742	3.0836
Set 3, $\phi_{ou}(u; x, \Delta t)$	3.3039	3.2822	3.2684
Set 3, $\phi_{app}(u; x, \Delta t)$	2.8212	2.8271	2.8084

Table 4
CPU time and error with parameter set at boundary of FFT and non-FFT ranges.

Sea. Fun.	Parameter	Set 1 $M = 10$	Set 1 $M = 50$	Set 2 $M = 20$	Set 2 $M = 40$
1	$\log_{10}$ (error)	−3.2217	−4.0466	−3.6035	−4.1734
	CPU time 1	15.7927	84.6543	33.1099	69.5744
	CPU time 2	0.0230	0.0769	0.0457	0.0702
2	$\log_{10}$ (error)	−3.5567	−4.4686	−3.4631	−4.1343
	CPU time 1	15.5535	84.7788	34.7118	74.6010
	CPU time 2	0.0232	0.0774	0.0454	0.0690

In Table 3 we see an increasing error in the early-exercise point, especially for parameters near the boundary of the range of κ- and σ-values for which the FFT can still be applied. With small parameter values for κ and σ, the error is relatively small (0.08 in Table 3).

Obviously, the Bermudan option prices with the approximate process are much more accurate than the values of the corresponding early-exercise points. This can be understood from Eq. (42) in our error analysis. There the error in the continuation value is divided by a small number (as $f'(x,t)$ is defined as the derivative of the difference of the continuation value and the payoff), resulting in a bigger error in ϵ_x, which is the error in the early-exercise points.

5.1.3. Seasonality experiment

Now we end with some test cases with seasonality. Our aim is to show that the approximation works well for different seasonality functions. Two seasonality functions are used:

1. Seasonality Function 1: $G(t) = 5 + \sin(t)$.
2. Seasonality Function 2: $G(t) = 3 + 4\cos(0.25t)$.

We check two parameter sets at the boundary of the FFT range, see Fig. 1 and Fig. 3.

1. Parameter Set 1: $\kappa = 1.5$, $\sigma = 0.8$, $T = 1$.
2. Parameter Set 2: $\kappa = 0.85$, $\sigma = 0.7$, $T = 2$.

CPU time as well as the log-absolute error in the option price from our approximate model for different M are presented in Table 4. For these parameter sets at boundary, we cannot achieve basis point precision for small values of M. However, the error drops below the tolerance level as M increases, which is in accordance with our analysis.

6. Conclusion

In this paper, we derive a characteristic function for an approximation of the well-known OU process. This approximation enables us to apply the Fast Fourier Transform when pricing Bermudan options by means of the COS method. The approximate process may be employed if the error generated by the approximation is less than a prescribed tolerance level. We would like to ensure that the Bermudan option prices are accurate up to a basis point. This tolerance level is determined by a detailed error analysis. In various numerical experiments it is demonstrated that the characteristic function for the approximate process, in combination with the tolerance level, predicts well for which model parameter ranges, numbers of early-exercise dates and seasonality functions the FFT can be safely applied. Moreover also the value of Delta is obtained with basis point precision in the FFT range. For the model parameter sets for which the error is below the tolerance level and our approximation can thus be applied, we have reduced the computational time for pricing of Bermudan options under the OU process from seconds to milliseconds.

References

[1] O.E. Barndorff-Nielsen, Normal inverse Gaussian distributions and stochastic volatility modelling, Scand. J. Statist. 24 (1997) 1–13.
[2] C. Blanco, D. Soronow, Mean reverting processes – Energy price processes used for derivatives pricing and risk management, Commodities Now, Energy Pricing, 2001.

[3] N. Branger, O. Reichmann, M. Wobben, Pricing electricity derivatives, Working Paper, 2009.
[4] P.P. Carr, H. Geman, D.B. Madan, M. Yor, The fine structure of asset returns: An empirical investigation, Journal of Business 75 (2002) 305–332.
[5] U. Cartea, M.G. Figueroa, Pricing in electricity markets: A mean reverting jump diffusion model with seasonality, Applied Mathematical Finance 12 (4) (2005) 313–335.
[6] R. Cont, P. Tankov, Financial Modelling with Jump Processes, Chapman and Hall, Boca Raton, FL, 2004.
[7] M. Dahlgren, A continuous time model to price commodity-based swing options, Review of Derivatives Research 8 (2005) 27–47.
[8] D. Duffie, J. Pan, K. Singleton, Transform analysis and asset pricing for affine jump-diffusions, Econometrica 68 (2000) 1343–1376.
[9] F. Fang, C.W. Oosterlee, A novel option pricing method based on Fourier-cosine series expansions, SIAM J. Sci. Comput. 31 (2) (2008) 826–848.
[10] F. Fang, C.W. Oosterlee, Pricing early-exercise and discrete barrier options by Fourier-cosine series expansions, Numer. Math. 114 (2009) 27–62.
[11] J. Hull, A. White, Pricing interest-rate derivative securities, Rev. Fin. Studies 3 (1990) 573–592.
[12] S.G. Kou, A jump diffusion model for option pricing, Management Science 48 (8) (2002) 1086–1101.
[13] J.J. Lucia, E.S. Schwartz, Electricity prices and power derivatives: Evidence from the Nordic power exchange, Review of Derivatives Research 5 (2002) 5–50.
[14] D.B. Madan, P.R. Carr, E.C. Chang, The Variance Gamma process and option pricing, European Finance Review 2 (1998) (1998) 79–105.
[15] R. Merton, Option pricing when underlying stock returns are discontinuous, Journal of Financial Economics 3 (1976) 125–144.
[16] E.S. Schwartz, The stochastic behavior of commodity prices: Implications for valuation and hedging, Journal of Finance 54 (3) (1997) 923–973.
[17] E.S. Schwartz, Valuing long-term commodity assets, Financial Management 27 (1998) 57–66.
[18] E.S. Schwartz, J.E. Smith, Short-term variations and long-term dynamics in commodity prices, Management Science 46 (2000) 893–911.
[19] G.E. Uhlenbeck, L.S. Ornstein, On the theory of Brownian motion, Phys. Rev. 36 (1930) 823.